Evolution of Properties of an Isocyanate/Epoxy Thermosetting System During Cure: Continuous Heating (CHT) and Isothermal Time–Temperature–Transformation (TTT) Cure Diagrams

M. T. DEMEUSE,[1,*] J. K. GILLHAM,[2] F. PARODI[3]

[1] EniChem America Inc., 2000 Cornwall Road, Monmouth Junction, New Jersey 08852

[2] Department of Chemical Engineering, Princeton University, Princeton, NJ 08544

[3] EniChem SpA, Via Fauser 4, I-28100, Novara, Italy

Received 3 July 1996; accepted October 31, 1996

ABSTRACT: The present article describes a methodology for examining the evolution of the properties vs. cure of a complex thermosetting isocyanate/epoxy reactive mixture which reacts through two consecutive but separable reaction regimes. The methodology is based on the use of the torsional braid analysis (TBA) technique and the continuous heating (CHT) and isothermal time–temperature–transformation (TTT) cure diagrams. © 1997 John Wiley & Sons, Inc. J Appl Polym Sci **64:** 15–25, 1997

Key words: Isocyanate/epoxy thermosetting system; cure; transitions; CHT cure diagram; TTT cure diagram; torsional braid analysis (TBA)

INTRODUCTION

Gelation and vitrification are the two principal events which can occur during the chemical transformation (cure) of a reactive thermosetting fluid to a glass. This work pertains to the development of a general methodology for characterizing the cure behavior of complex thermosetting systems without explicit knowledge of the chemistry. The approach is to produce and use two cure diagrams. The continuous heating time–temperature–transformation (CHT) cure diagram[1] is obtained by heating, at different heating rates, an initially unreacted formulation from below its initial glass transition temperature, T_{g0}, to above its maximum glass transition temperature, $T_{g\infty}$. This involves using one specimen for each heating rate. The temperatures of events (transitions) are obtained as the material changes from an unreacted sol glass to sol liquid, to sol gel rubber (through gelation), to sol gel glass (through vitrification), to gel glass, and to gel rubber; events due to thermal degradation are also likely to be encountered. The CHT cure diagram has temperature as the y-axis and log time as the x-axis. The isothermal time–temperature–transformation (TTT) cure diagram[2] is obtained by isothermal heating of initially unreacted formulations to obtain the time to gel and the time to vitrify. This involves using one specimen for each isothermal temperature. The TTT diagram has the temperature of cure, T_{cure}, as the y-axis and log time as the x-axis. The time to vitrify in the TTT diagram is generally an S-shaped contour for simple step-growth thermosetting reactions.[3] The time to gel is a decreasing exponential function with increasing temperature according to Flory's gelation theory.[4]

Correspondence to: J. K. Gillham.

* *Present address:* AET Packaging Films, Hercules Research Center, 500 Hercules Road, Wilmington, DE 19808.

In the past, the above ideas have been applied principally to model systems of commercial interest for which there was considerable knowledge already available about the chemical reactions and their kinetics. The TTT and CHT diagrams provide a framework for understanding the cure of thermosetting systems in providing relationships among reactivity, processing, and properties during cure. Recently,[5] a conversion–temperature–property diagram was introduced which treats the relationship between the extent of cure and isothermal material properties over a range of isothermal temperatures. The present work deals with a complex experimental thermosetting system for which a knowledge of the chemistry is incomplete and demonstrates the extent to which an understanding of the processing[6,7] and properties[8] can be gained without an explicit understanding of the chemistry.

The unreacted formulation (Fig. 1) is a mixture of excess diisocyanate, a diepoxide, and a catalyst. Such a mixture can react and generate crosslinked polymeric material through formation of heterocyclic isocyanurate and oxalidine-2-one (or simply 2-oxazolidone) moieties.[9,10] Isocyanurates derive from the cyclotrimerization of isocyanates, a reaction which is strongly co-catalyzed by epoxides, whereas five-membered 2-oxazolidone rings are produced by the 1,3-cycloaddition of an isocyanate with an epoxy group (yielding both the isomeric 3,5- and 3,4-disubstituted oxazolidine-2-one structures)[11] (Fig. 1).

Catalysts suitable for the synthesis of 2-oxazolidones in high yields have included mild nucleophilic agents, such as halide ions, alkali or alkaline-earth metal halides in dipolar aprotic solvents, tertiary amines, as well as complexes of Lewis acids (e.g., $AlCl_3$) with a Lewis base excess (e.g., a tertiary amine or phosphine, or a tertiary phosphine oxide).[12–16] The catalyst used in the present work is shown in Figure 1. According to an accepted reaction pathway, the 2-oxazolidation proceeds via the nucleophilic attack of the catalyst on the epoxy ring. It generates a new active species, bearing a nucleophilic center, that causes 2-oxazolidone formation by the general mechanism of cycloaddition of isocyanates.[11] The active intermediate can also promote isocyanurate production by the known mechanism of the epoxy-cocatalyzed cyclotrimerization of isocyanates.[11] Other, unknown, thermal degradation reactions occur at high temperatures.

The two processes of isocyanurate and 2-oxazolidone formation compete with each other to form crosslinked structures. Their rates and the resulting amounts of the two moieties are governed by many parameters: e.g., isocyanate-to-epoxy ratio, catalyst type and concentration, chemical structure of reactants, and temperature. Moreover, a third process is catalyzed by the nucleophilic agent: 2-oxazolidones can be indirectly formed by an isocyanurate–epoxy rearrangement reaction[15,16] (see Fig. 1). This reaction leads to a decrease in crosslink density.

The stiff and bulky isocyanurate and 2-oxazolidone moieties strongly contribute to the high glass transition temperature values of the polymeric materials[17] and inherently possess good thermal stabilities.[18] Based on such features, suitably catalyzed systems of liquid aromatic polyisocyanates

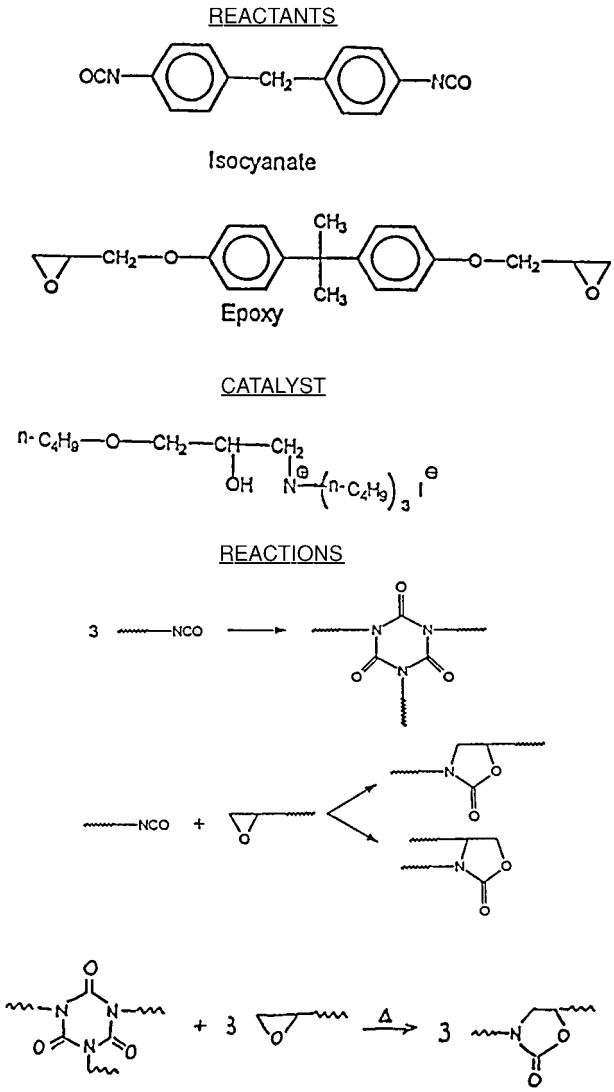

Figure 1 Chemical reactants, catalyst, and overall reactions.

and di- or polyfunctional epoxy resins (primarily polyisocyanates of the diphenylmethane group and diglycidyl ethers of bisphenols or novolacs) are being proposed as thermosetting resins for high-temperature applications.[17,19,20]

Examples of these applications are casting resins for molding or embedding electrical devices[21,22] and encapsulation of electronic devices,[23,24] laminates for printed circuit boards,[25] and adhesives.[26] The curing of such resins is typically accomplished by heating for 0.5–8 h at temperatures from 80 to 150°C. Fast-curing isocyanate/epoxy compositions, with hardening times of only minutes at temperatures below 100°C, have also been developed for generation of cellular materials[27] and for fabrication of advanced composites by the resin transfer molding and structural reaction injection molding techniques.[28]

The multiplicity of chemical reactions through which these resins cure has been investigated by differential scanning calorimetry and infrared spectroscopy.[10,29,30] A general indication arising from these studies is that temperature is the dominant variable which controls the occurrence of the various reactions. They tend, in fact, to take place in a precise succession when cure is performed, as is frequently done, by a temperature ramp: The polymerization begins with the isocyanate trimerization, which is followed by direct 2-oxazolidation and then, only at high temperatures, by the isocyanurate/epoxy "rearrangement" to further 2-oxazolidone (Fig. 1).

Despite the interest displayed in the isocyanate/epoxy type of resins for many years, no special attention has been focused on the evolution of physical properties during polymerization. The present manuscript deals with the CHT and TTT diagrams. A parallel manuscript deals with the evolution from brittle to tough material with increasing extent of cure.[8] These diagrams are obtained using the experimental technique of torsional braid analysis (TBA).[31–33]

EXPERIMENTAL

The isocyanate used in these studies is a liquid urethonimine-modified diphenylmethane diisocyanate (70 parts by weight) with an average isocyanate functionality of 2.15 and an equivalent weight of 147.9 g/equiv. It was supplied by the Polyurethanes Division of EniChem SpA. Its viscosity at 25°C is 50 cPs. The epoxide portion of the mixture is a diglycidyl ether of bisphenol A (Dow Chemical Co., DER 330; 29.5 parts by weight) with a theoretical epoxy functionality of 2.0 and an epoxy equivalent weight of 182.4. The catalyst is [(2-hydroxy-3-*n*-butoxy)propyl]tri-*n*-butylammonium iodide (0.5 parts by weight).[34] The stoichiometry is such that an excess of isocyanate is present; mol of isocyanate groups/mol of epoxide groups = 2.8/1.0. The structures of the three chemicals and the proposed reactions[9–11] are shown in Figure 1. The initial information which was available concerning the formulation was that the mixture had a gel time at 40°C of about 30 min.

Dynamic mechanical experiments were conducted using the torsional braid analysis (TBA)[31–33] technique which is a freely oscillating torsion pendulum with a composite specimen made by impregnating a glass braid substrate with a reactive fluid. The TBA unit is used to monitor the dynamic mechanical behavior of the specimen at approximately 1 Hz between −180 and 400°C. The formulation was prepared by adding a mixture of liquid diisocyanate and catalyst to the diepoxide at room temperature and thoroughly mixing by stirring for 3 min. The reactive liquid formulation was used to impregnate a heat-cleaned glass braid to form a specimen for the TBA torsion pendulum experiment. Excess material on the braid was removed by squeezing the impregnated braid between aluminum foil. The final amount of material on the braid was approximately 15 mg.

The pendulum is set intermittently into free vibration to generate a series of freely damped waves, each of which is characterized by its frequency (Hz = $1/P$, where P = period of oscillation in seconds) and a decay constant. The relative shear modulus (G') of the specimen is given by the square of the frequency and is designated "rigidity" or "relative rigidity." The mechanical damping of the specimen is given by either the logarithmic decrement ("log decrement") ($\Delta = \pi \times G''/G'$) or the loss shear modulus (G''). Transitions are assigned from maxima in the mechanical damping. All experiments in the TBA unit were performed in an atmosphere of flowing helium.

For experiments used to construct the CHT diagram, a specimen, after having been prepared and mounted between two vertical rods (part of the inner TBA pendulum assembly), was lowered into the TBA chamber which had been preset at 15°C and quenched at 7.5°C/min to −50°C, and then heated at a constant heating rate to 325°C before cooling at 2°C/min to below T_g. A CHT diagram

was constructed from the data obtained on heating different specimens from −50 to 325°C at different rates.

Two different types of experiments were performed with respect to the isothermal TTT cure diagram. The first, after lowering the inner TBA pendulum assembly into the TBA unit at −15°C and cooling to −50°C, involved repetitive heating of a single specimen from −50°C at 2°C/min to an isothermal temperature, T_{cure} (range = 25–125°C), holding at the isothermal temperature—for longer times for successive cycles, cooling to −50°C at 7.5°C/min, and holding for 5 min at −50°C before repeating numerous times the heating, holding at the isothermal temperature, cooling, and holding at −50°C. This experiment allowed an evaluation of the increase of T_g with isothermal hold time to be made using the assumption that cure was advanced only at T_{cure}. A different specimen was used for each isothermal temperature.

A second type of isothermal experiment involved heating the temperature chamber of the TBA unit to a preset temperature, T_{cure}. An unreacted specimen was rapidly lowered into the temperature chamber at T_{cure}. The isothermal increase in rigidity (G') and the change in mechanical damping of the specimen vs. time were monitored. Gelation and vitrification were determined from the peaks in the mechanical damping. The isothermal curing experiments were performed for 10 h. The automated TBA system is available from Plastics Analysis Instruments, Inc., Princeton, NJ.

RESULTS AND DISCUSSION

CHT Diagram

An example of a TBA scan from −50 to 325°C is shown in Figure 2. Transition temperatures are assigned from this plot from the temperatures of maxima in the logarithmic decrement vs. temperature. The sequence of events, from the damping maxima, is T_{g0} (the initial glass transition temperature of the reactants); $T_{\ell\ell}$ and T_{gel} [which correspond to an isoviscous state ($\eta > 10{,}000$ cPs)][31]; an undesignated event beyond gelation; T_{vit} (which corresponds to vitrification (i.e., $T_g = T$); and T_g (which corresponds to the maximum glass transition temperature measured on heating). Another undesignated event is discernable between $T_{\ell\ell}$ and T_{gel} by a shoulder in the mechanical loss.

The interval $T_{gel} - T_{\ell\ell}$ is a measure of the "window" for processing in the liquid state. The viscosity between $T_{\ell\ell}$ and T_{gel} is < 10,000 cPs.[31] The interval between T_{gel} and the end of the rubbery region ("ETR") is a measure of the width of the rubbery state after gelation. The end of the rubbery region is obtained from a linear extrapolation of the linear rigidity data prior to vitrification to zero rigidity. The large temperature interval between gelation and the onset of vitrification suggests that there are two consecutive and separable reaction regions.

The CHT diagram of Figure 3 summarizes the results for the different heating rates. Numerical data for the transition events vs. heating rate are shown in Table I. Initial devitrification ($\sim T_{g0}$), vitrification (T_{vit}), and final devitrification (T_g) appear to form an S-shaped contour. $T_{\ell\ell}$ and T_{gel} events appear to form parts of a reverse-C contour (corresponding to isoviscosity events). Different states are sol glass, sol liquid, sol gel rubber, gel rubber (not marked), sol gel glass, degraded gel rubber (not marked), gel glass (not marked), and degraded gel glass (not marked).

The principal transitions, which are characteristic of the particular thermosetting system, are $T_{g0} = -35$°C, ${}_{gel}T_g < 34$°C, and $T_{g\infty} > 315$°C (see later). ${}_{gel}T_g$ is less than 34°C as measured from the temperature of intersection of the extrapolated gelation contour and the extrapolated vitrification contour.[2,31] Another specimen, heated at 2°C/min to the maximum in the logarithmic decrement corresponding to T_{gel} and quenched before reheating, gave a value of ${}_{gel}T_g = 39$°C, which is considered to be a maximum value for ${}_{gel}T_g$.

It is noted, as expected, that the widths of the temperature region for liquid processing ($T_{gel} - T_{\ell\ell}$) and for the rubbery state (ETR − T_{gel}) increase with heating rate. There is uncertainty in extrapolating the vitrification contour to slower rates than 0.075°C/min because of later findings.

Figure 3 also includes the glass transition temperature, ${}^{325}T_g$, measured during cooling at 2°C/min from 325°C after heating at different heating rates to 325°C. On heating to 325°C, there is a competition between cure which increases T_g and thermal degradation which decreases T_g. This leads to T_g passing through a maximum. $T_{g\infty}$ would be expected to be higher than the highest value of T_g measured on heating. (From the CHT diagram, $T_{g\infty} > 315$°C.) This is consistent with the data that show that for slow heating rates the

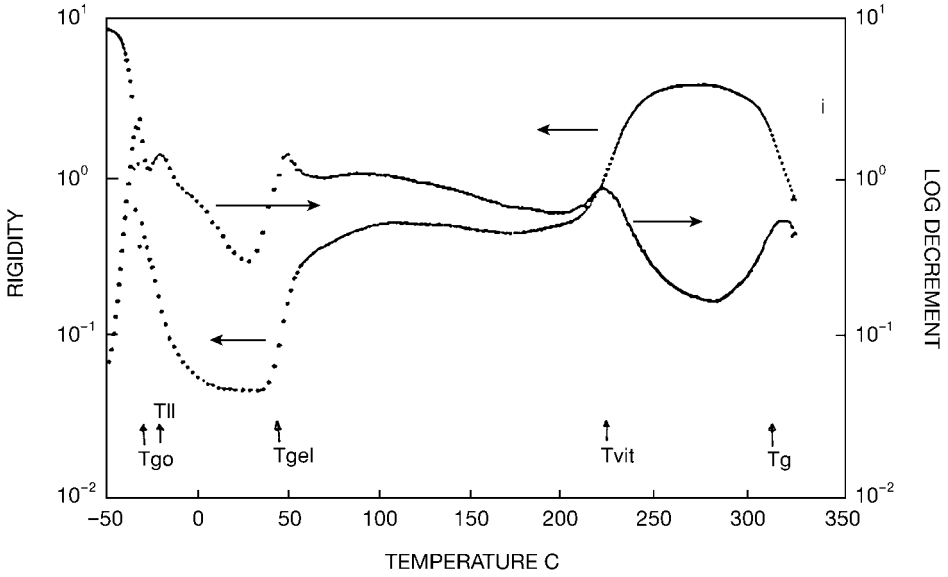

Figure 2 Rigidity and log decrement vs. temperature at 1°C/min. Vertical arrows mark the events (see text).

differences between T_g (on heating) and T_g (on cooling) decrease with decreasing heating rate due to the majority of the degradation occurring on heating to 325°C. At fast heating rates to 325°C, the maximum value of T_g will not be obtained because the system is not provided adequate time to fully react.

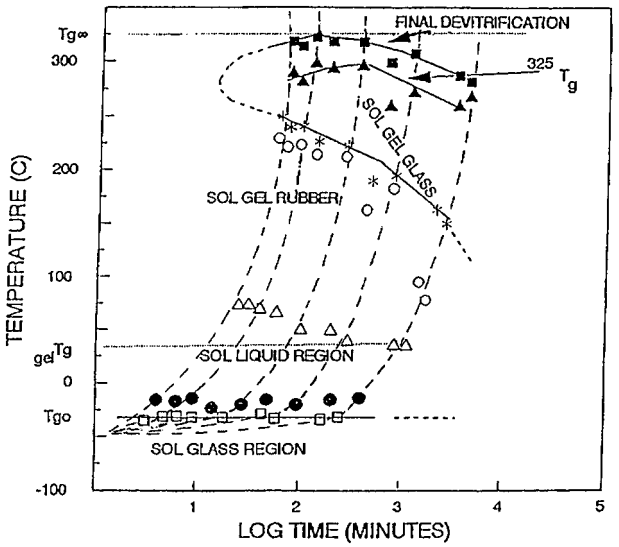

Figure 3 CHT diagram. Full lines connect data points for initial devitrification ($\sim T_{g0}$), for vitrification ($T_g = T$), for final devitrification ($T = T_g$), and for $^{325}T_g$ (see text). Dotted contours represent temperature vs. log time at several heating rates. Note: Only some of the different states are listed (see text). (□) T_{g0}; (●) $T_{\ell\ell}$; (△) T_{gel}; (○) end of rubbery region; (*) T_{vit}; (■) T_g; (▲) $^{325}T_g$.

The CHT diagram has the advantage of being a relatively simple way for obtaining the different regions of behavior of a reactive system vs. temperature. (For example, as reported here, nine specimens were used and generated the data within 10 days.) It is more conveniently obtained for an unknown reactive system than for the corresponding isothermal TTT diagram, since the various transitions which occur during heating from below T_{g0} to above $T_{g\infty}$ are immediately revealed, whereas the gelation and vitrification events of the isothermal TTT diagram can only be obtained experimentally for restricted isothermal temperatures for experimental reasons which include the isothermal reactivity of the formulation at different temperatures.

However, the CHT diagram, as generated, has some ambiguities. For example, although it appears that a contour connecting initial devitrification, vitrification, and final devitrification forms an S-shaped contour, reasonable extrapolation to slow heating rates cannot be made. Also, it is not clear how the two reaction regions converge at long times and relatively low temperatures ($\sim$ 100°C). Further elucidation of the latter is provided using the TTT diagram.

Other investigations, based on differential scanning calorimetric and infrared spectroscopic methods, did not reveal such a clear reaction separation for a variety of isocyanate/epoxy systems.

Table I Transition Events vs. Heating Rate

Heating Rate (°C/min)	T_{g0} (°C)	T_{γ} (°C)	T_{gel} (°C)	ETR (°C)	T_{vit} (°C)	T_g (°C)
0.075	−32	−19	34	78	~ 150	279, 284
0.1	−34	−19	34	95	~ 163	287
0.3	−33	−20	38	183	~ 195	307
0.5	−28	−18	49	163	~ 190	299
1.0	−32	−21	50	213	223	318
2.0	−32	−22	66	215	227	318
3.0	−31	−14	69	224	241	323
4.0	−31	−18	73	222	240	314
5.0	−34	−21	73	230	250	318

For example, such a situation was not observed with many 2-ethyl-4-methylimidazole-catalyzed systems using a heating rate of 20°C/min[28] or a series of uncatalyzed systems at a heating rate of 1.8°C/min.[29] A two-stage curing process has been disclosed for some practical applications of isocyanate/epoxy resins, as in the preparation of prepregs for fiber-reinforced laminates (e.g., printed circuit boards)[24] and with casting resins and resin compounds for molding or encapsulation of electrical/electronic components.[22,24] In these cases, indeed, the resin is reacted at moderate temperatures (100–130°C) and then cooled to give a viscous liquid or a low T_g glassy prepolymer, having a high isocyanate content. The product is claimed to be storage-stable, still soluble and moldable, and can be rapidly hardened above 160°C to the final high T_g material.[35] It is not clear from those reports whether the disclosure of such a two-stage cure is a consequence of the knowledge of consecutive reactions or simply the quenching of the partially cured material.

It was decided to address the experimental findings from the CHT diagram with respect to the two-stage reaction regimes by performing a series of isothermal experiments. This is the methodology of the isothermal time–temperature–transformation (TTT) cure diagram.[2] The two stages of the reaction are presumed to yield, correspondingly, two maximum glass transition temperatures, $T_{g1\infty}$ ($\simeq$ 110°C from the TTT diagram) and $T_{g2\infty}$ ($\equiv T_{g\infty} >$ 315°C from the CHT diagram).

TTT Cure Diagram

Isothermal T_g vs. time plots were obtained at different temperatures using the TBA system in an attempt to extract a master curve for chemical kinetic control of conversion (T_g) vs. time at an arbitrary temperature and an activation energy from the shift factors used to produce the master curve. The procedure assumes that T_g is uniquely related to conversion (which is not shown explicitly in this work). From this information, isoconversion (T_g) contours for the TTT diagram can be computed. If it is also assumed that kinetic control extends to the point of vitrification ($T_g = T_{cure}$), then the vitrification contour can also be computed (as below). If gelation occurs at a definite and known or calculable conversion (e.g., as in Flory's simplest theory of gelation), an iso-T_g gelation contour can be calculated for the TTT diagram. The methodology develops that used earlier.[1,2]

Figure 4 contains the experimental glass transition temperature vs. time of curing data for isothermal temperatures which range from 25 to 125°C following the procedures outlined above. The use of this procedure assumes that the reaction occurs at T_{cure} and that no reaction occurs during the heating and cooling portions of the cycle. The measurement of T_g was made during heating to T_{cure} using the maximum in the loss modulus data. The loss modulus rather than logarithmic decrement was used because the assignment of T_g from the latter is complicated during the early stages of polymerization by the $T_{\ell\ell}$ transition.[2,31]

By treating the data as if the reaction is only kinetically controlled, the reaction rate, dx/dt, can be described mathematically by the kinetic rate equation

$$dx/dt = k(T) \times f(x) \qquad (1)$$

where $k(T)$ is the reaction rate constant that is

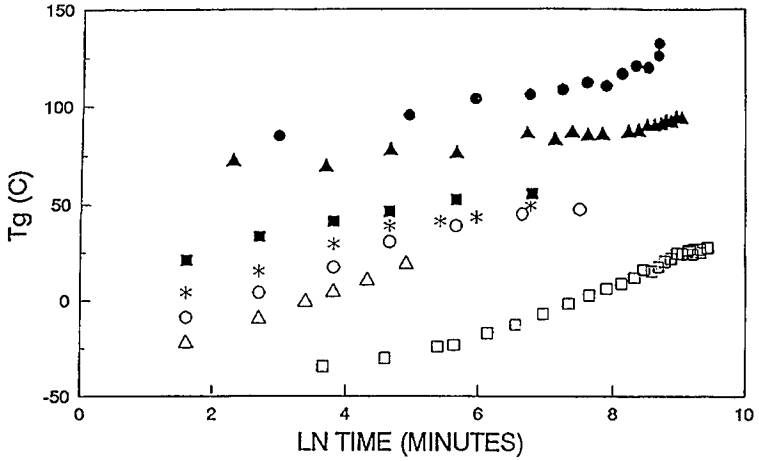

Figure 4 Experimental glass transition temperature (T_g) vs. ln time of curing at isothermal temperatures from 25 to 125°C. (□) T_{cure} = 25°C; (△) 40°C; (○) 45°C; (*) 50°C; (■) 55°C; (▲) 100°C; (●) 125°C.

a function of temperature, T, only; $f(x)$ is some function of conversion, x; and t is the cure time.

Rearranging eq. (1), integrating at constant temperature, and taking the natural logarithm produces

$$\ln\left[\int_0^x dx/f(x)\right] = \ln k(T) + \ln(t) \qquad (2)$$

The left-handed side of this equation is a function of conversion only and, equivalently, therefore, a function of T_g only, i.e., $F(T_g)$ (assuming a one-to-one relationship between conversion and T_g). Therefore,

$$F(T_g) = \ln k(T) + \ln(t) \qquad (3)$$

This equation describes the variation of T_g with cure time and temperature.

Let T_g vary with time t_1 for cure temperature T_1, and with time t_2 for cure temperature T_2:

$$F(T_g) = \ln k(T_1) + \ln(t_1) = \ln k(T_2) + \ln(t_2) \qquad (4)$$

$$\ln(t_1) - \ln(t_2) = \ln k(T_2) - \ln k(T_1) \qquad (5)$$

For any two isothermal temperatures, $\ln k(T_2) - \ln k(T_1)$ is a constant. Therefore, for a kinetically controlled reaction, the variation of T_g with time at two different cure temperatures (T_1 and T_2) when plotted as a function of ln(time) will have the same functional form except that the curve for the cure temperature T_2 will be displaced from that of the temperature T_1 by a constant factor. It follows that if the reaction is solely kinetically controlled, all T_g vs. ln(time) curves at different cure temperatures should be superimposable by shifting each curve along the ln(time) axis relative to a curve at an arbitrary reference temperature by a shift factor, $A(T) = \ln(t_{ref}) - \ln(t_T)$, for each temperature relative to the reference temperature.

The isothermal data of T_g vs. time at different temperatures were shifted along the ln time scale to produce a master curve at an arbitrary reference temperature of 45°C. The shift factors, $A(T_{cure})$, were obtained operationally by superimposing short time data. Figure 5 contains a plot of the shift factor, A, vs. $1/T$ (K), assuming an Arrhenius relationship [i.e., $A(T_{cure})$ = constant × $\exp(-E/RT)$]. For a kinetically controlled reaction mechanism, the temperature dependence of the rate constant is generally given by an Arrhenius relationship:

$$k(T) = A_0 \exp(-E/RT) \qquad (6)$$

where all parameters have the usual Arrhenius significance and T is in units of absolute Kelvin.

The shift factors can be used to calculate the Arrhenius activation energy for the reaction since eq. (5) provides the relationship between the time shift factors and the rate constants:

$$A(T) = \ln(t_{ref}) - \ln(t_T) = \ln k(T) - \ln k(T_{ref}) = -E/RT + E/RT_{ref} \qquad (7)$$

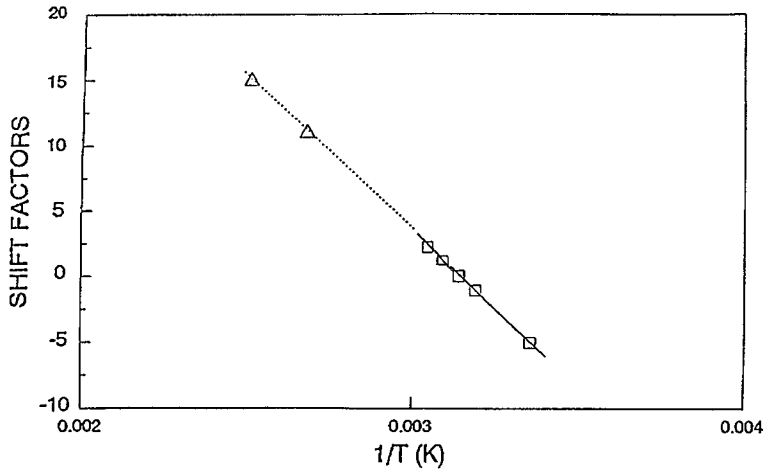

Figure 5 Plot of shift factor vs. $1/T$ (K) to determine apparent activation energy. (□) Actual shift factors; (△) extrapolated shift factors for temperatures of 100 and 125°C.

When T_{ref} is fixed and all other data are shifted relative to the reference temperature, plotting the shift factor vs. $1/T(K)$ should yield a straight line with the slope given by $-E/R$ and intercept equal to $E/(RT_{\text{ref}})$.

A value of the apparent activation energy equal to 47 kcal/mol was obtained from the slope of the straight line for the data from 25 to 55°C. This straight line was then extrapolated to 100 and 125°C to obtain the shift factors for these temperatures which were used to shift the data at 100 and 125°C onto the master curve. Note that direct experimental data at 100 and 125°C could not be obtained for short times because of the high reaction rate.

The master curve for the first reaction region is displayed in Figure 6. A note with respect to diffusion control: Some of the isothermal data were obtained when $T_g > T_{\text{cure}}$. If diffusion control had occurred at vitrification, then data beyond vitrification would not have fitted on the master curve. This implies that all the data were under kinetic control.

The short-time data at 100 and 125°C lie on the same master curve as do the lower-temperature data. It follows that either (1) there is only a single reaction below 125°C or (2) different reactions have the same apparent activation energies. Also, the upturn in the data at long times at 125°C suggests the onset of the occurrence of a second reaction.

The master curve and the activation energy provide sufficient information for calculating iso-T_g vs. time contours and the time to vitrify contour.[2] The basic assumptions in the calculation are that (1) the reaction prior to vitrification is kinetically controlled and (2) there is a one-to-one relationship between T_g and chemical conversion.

The relationship between the times to reach a fixed T_g at different cure temperatures for a kinetically controlled reaction is given by eq. (7), recast as follows:

$$-E/RT_1 + \ln(t_{T_g,1}) = -E/RT_2 + \ln(t_{T_g,2}) \quad (8)$$

where $t_{T_g,1}$ is the time needed to reach a given glass transition temperature T_g, at cure temperature T_1, and $t_{T_g,2}$ is the time needed to reach the same T_g value at cure temperature T_2. Thus, if a time to reach a particular T_g at one particular cure temperature (i.e., $t_{T_g,1}$ at T_1) is known, then the times to reach the same T_g at different temperatures (i.e., $t_{T_g,2}$ at any T_2) can be calculated from eq. (8) provided that the reaction activation energy is available. The times to reach a fixed T_g at different cure temperatures, when plotted as T_{cure} vs. cure time, constitute an iso-$T_g = T_g$ line in the TTT cure diagram. To calculate all possible iso-T_g contours, data points relating $T_g - t_{\text{cure}} - T_{\text{cure}}$ under kinetically controlled conditions over the entire range of T_g are required.

When T_2 is equal in value to the glass transition temperature, T_g, the time $t_{T_g,2}$ calculated from eq. (8) is the time to reach isothermal vitrification when the material is cured at the T_g value. Vitrification points for all possible values of T_g (i.e., from $T_g = T_{g0}$ to $T_g = T_{g\infty}$), when plotted in the

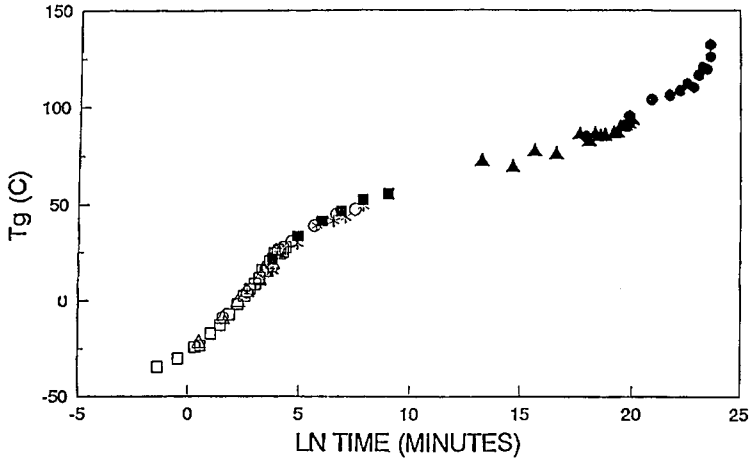

Figure 6 Master curve for T_g vs. time data. (□) T_{cure} = 25°C; (△) 40°C; (○) 45°C; (*) 50°C; (■) 55°C; (▲) 100°C; (●) 125°C.

form of T_{cure} vs. cure time, constitute the vitrification curve in the TTT diagram.

Values of $T_{g0} = -35$°C and $T_{g1\infty} = 110$°C were used to generate the TTT diagram for the first reaction regime. If gelation occurred at a fixed chemical conversion, the time to gel would correspond to an iso-T_g contour at $T_g = {}_{gel}T_g$ in the TTT diagram. Estimates of ${}_{gel}T_g$ were obtained in the generation of the CHT diagram.

Having generated a TTT diagram, as above, for the first reaction region, isothermal experiments were performed in an attempt to directly confirm the times to vitrification in the temperature range 25–110°C. Gelation was assigned from the peak in the logarithmic decrement ($=\pi$ tan delta) data whereas vitrification was assigned from the peak in the loss modulus data.

Figure 7 contains a comparison of calculated isothermal vitrification times with the experimentally determined isothermal vitrification times for the first reaction region. Note that the times to gel above 60°C were too short to measure directly. The slope of the straight line of an Arrhenius plot of the ln time to gelation vs. $1/T$ (K) yields a value of 16.4 kcal/mol for the apparent activation energy of the reactions leading to gelation. Note that this value is different from the value of the apparent activation energy which was obtained from the shift factors for the master curve of T_g vs. ln time. It may be due to (1) that gelation, as measured by TBA, is an isoviscous event, not an isoconversion event,[2,31] or (2) that the assumption that T_g relates one-to-one to conversion is not applicable to this system. However, it is noted that the quality of the gelation data is not good.

Figure 8 contains the entire TTT diagram, including the times to vitrify vs. T_{cure} from T_{g0} to $T_{g2\infty}$. Data above $T_{g1\infty}$ were obtained by direct isothermal experimentation whereas data below $T_{g1\infty}$ include both experimental and calculated data. The experimental times to gelation for isothermal temperatures are shown from 25 to 50°C. Two S-shaped vitrification curves are shown. The first corresponds to a low temperature reaction region (calculated and limited direct experimental data). The second S-shaped contour corresponds to a high-temperature reaction region with vitrification data obtained by direct measurement. Critical temperatures are $T_{g10} = -35$°C, $T_{g1\infty} = 110$°C, and $T_{g2\infty} > 315$°C. Note that $T_{g20} = T_{g1\infty}$.

The complex form of the vitrification contour is based on the supposition of two consecutive and separable reaction regions which was first deduced from the wide rubbery region seen in the temperature scans using rapid (e.g., 1°C/min) heating rates of the CHT diagram. If there are two separate reaction regions, there should be two T_g's to consider, one being connected with the low-temperature reaction region and the other being connected with the high-temperature reaction region. Normally, with consecutive and separable reactions, the first reaction would be expected to go to completion giving a $T_g = T_{g1\infty}$, with the reaction via the second mechanism increasing $T_{g1\infty}$ to eventually $T_{g2\infty}$. The development of the glass transition temperature with cure was investigated using temperature scans after isothermal experiments in the region of overlap of the two reactions; this will form the basis of a further report.

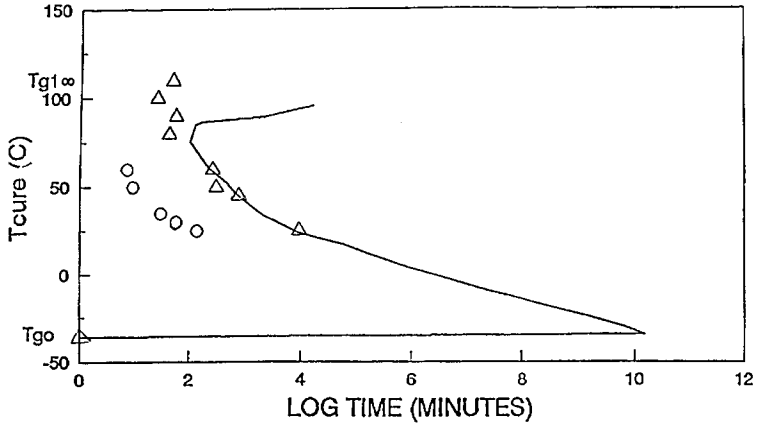

Figure 7 Isothermal TTT cure diagram for first reaction. (Full line) calculated; (△) experimental times to vitrify vs. isothermal temperature for the first reaction region; (○) also, experimental times to gel.

CONCLUSIONS

The CHT diagram has been generated for the particular thermosetting system. The principal transitions are $T_{g0} = -35°C$, $_{gel}T_g < 34°C$, and $T_{g\infty} > 315°C$. Two particular regions of the diagram have been identified: (1) the limited temperature width of the liquid region which will affect processability and (2) the extensive temperature width of the rubbery region between sharp increases in modulus, which suggests two consecutive and separable reaction regions.

The isothermal time–temperature–transformation (TTT) cure diagram has also been generated for the particular thermosetting system. The diagram is interpreted on the basis of there being two consecutive and separable reactions which lead to isothermal vitrification. The first reaction results in $T_{g1\infty} = 110°C$ and the second reaction results in $T_{g2\infty} > 315°C$ ($\equiv T_{g\infty}$, CHT diagram). The gelation times have been explicitly determined experimentally for cure temperatures ranging from 25 to 50°C: above 50°C, the reaction occurs too rapidly for gelation to be experimentally measured. The vitrification contour has been studied in two ways. For low temperatures, a master curve has been generated for the first reaction region. Knowledge of the master curve and the apparent activation energy value allowed for calculation of the isothermal vitrification times for the first reaction region. Direct experimental determination of the isothermal vitrification times for these low temperatures provided a confirmation of the calculated vitrification times. Further experimental measurements of the vitrification times for the second higher temperature reaction provided the complete TTT diagram.

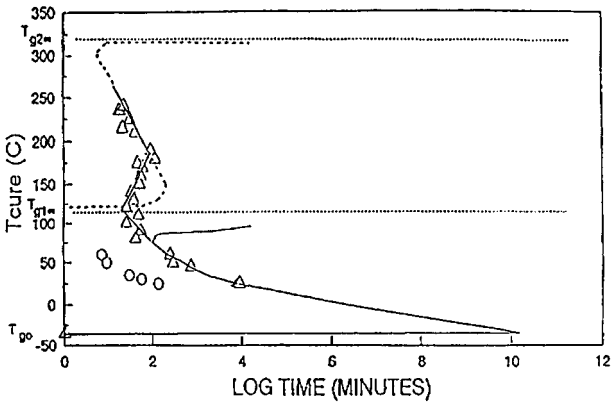

Figure 8 Isothermal TTT cure diagram. The time to vitrify vs. T_{cure} from T_{g0} to $T_{g2\infty}$; also, times to gel (○) (experimental) for lower isothermal temperatures. Two S-shaped vitrification curves are shown corresponding to a low-temperature (calculated with some experimental data) reaction region: (full line) calculated; (△) experimental; and a high-temperature reaction region: (dashed line) estimated; (△) experimental.

REFERENCES

1. G. Wisanrakkit and J. K. Gillham, *J. Appl. Polym. Sci.,* **42,** 2453 (1991).
2. G. Wisanrakkit and J. K. Gillham, *J. Appl. Polym. Sci.,* **41,** 2885 (1990).
3. M. T. Aronhime and J. K. Gillham, *J. Coat. Tech.,* **56,** 35 (1984).
4. P. J. Flory, in *Principles of Polymer Chemistry,* Cornell University Press, Ithaca, NY, 1953.

5. X. Wang and J. K. Gillham, *J. Appl. Polym. Sci.,* **47,** 425 (1993).
6. M. T. DeMeuse, J. K. Gillham, and F. Parodi, SAMPE, *Conference Proceedings,* Anaheim, 1994, p. 272.
7. M. T. DeMeuse, J. K. Gillham, and F. Parodi, SAMPE, *Conference Proceedings,* Anaheim, 1994, p. 286.
8. M. T. DeMeuse, J. K. Gillham, and F. Parodi, *J. Appl. Polym. Sci.,* **64,** 27 (1997).
9. A. A. R. Sayigh, *Adv. Urethane Sci. Technol.,* **3,** 141 (1974).
10. M. Uribe and K. A. Hodd, in *Advances in Polymer Synthesis,* B. M. Culbertson and J. E. McGrath, Eds., Plenum Press, New York, 1986, p. 251.
11. F. Parodi, in *Comprehensive Polymer Science,* G. C. Eastmond, A. Ledwith, S. Russo, and P. Sigwalt, Eds., Pergamon Press, Oxford, 1989, Vol. 5, p. 387.
12. G. P. Speranza and W. J. Peppel, *J. Org. Chem.,* **23,** 1922 (1958).
13. S. R. Sandler, *J. Polym. Sci. Polym. Chem. Ed.,* **5,** 1481 (1967).
14. M. Kitayama and R. A. Patsiga, *Rubb. Chem. Technol.,* **53,** 1 (1980).
15. A. Sendijarevic, V. Sendijarevic, and K. C. Frisch, *J. Polym. Sci. Polym. Chem. Ed.,* **265,** 151 (1987).
16. J. S. Senger, I. Yilgor, J. E. McGrath, and R. A. Patsiga, *J. Appl. Polym. Sci.,* **38,** 373 (1989).
17. N. Kinjo, S. I. Numata, T. Koyama, and T. Narahara, *J. Appl. Polym. Sci.,* **28,** 1729 (1983).
18. P. I. Kordomenos, J. E. Kresta, and K. C. Frisch, *Macromolecules,* **20,** 2077 (1987).
19. K. C. Frisch, A. Sendijarevic, V. Sendijarevic, and M. Vlajic, in *Proceedings of the 33rd SPI Polyurethane Conference,* Orlando, FL, Sept. 30–Oct. 3, 1990, p. 515.
20. J. Franke and H. P. Mueller, *Kunstoffe,* **80**(10), 1200 (1990); in *Proceedings of the Polyurethane World Congress 1991,* Nice, France, Sept. 24–26, 1991, p. 482.
21. H. Markert, W. Rogler, K. Kretzschmar, and W. Bendel, U.S. Pat. 4,564,651 (Jan. 14, 1986) (to Siemens A. G.); H. Markert, W. Rogler, and K. R. Hauschildt, U.S. Pat. 4,631,306 (Dec. 23, 1986) (to the Siemens A. G.).
22. H. P. Mueller, D. Kerimis, H. Heine, and W. Uerdingen, U.S. Pat. 4,728,676 (Mar. 1, 1988); H. P. Mueller, W. Uerdingen, and H. Heine, U.S. Pat. 4,788,224 (Nov. 29, 1988) (both to the Bayer A. G.).
23. K. Ishii and K. Suzuki, Jpn. Pat. 61-181,820 (Aug. 14, 1986) (to the Sumitomo Bakelite Co.).
24. H. P. Mueller and H. Heine, Ger. Pat. 3,807,660 (Sept. 13, 1989) (to the Bayer A. G.).
25. K. Suzuki and K. Ishii, Jpn. Pats. 57-003,812, 57-003,813 and 57-003,814 (Jan. 9, 1982). (to the Sumitomo Bakelite Co.).
26. A. B. Goel, U.S. Pat. 4,705,838 (Nov. 10, 1987) (to the Ashland Oil Inc.).
27. S. Fuzesi and R. W. Brown, U.S. Pats. 4,699,931 (Oct. 13, 1987) and 4,766,158 (Aug. 23, 1988) (to the Olin Corp.).
28. F. Parodi and C. Belgiovine, U.S. Pat. 5,145,880 (Sept. 8, 1992) (to the EniChem SpA).
29. Y. S. K. Lee, K. Hodd, W. W. Wright, and J. M. Barton, *Br. Polym. J.,* **22,** 97 (1989).
30. T. I. Kadurina, V. A. Prokopenko, and S. I. Omelchenko, *Polymer,* **33,** 3858 (1992).
31. J. K. Gillham, in *Developments in Polymer Characterisation-3,* J. V. Dawkins, Ed., Applied Science, London, 1982, pp. 159–227.
32. J. B. Enns and J. K. Gillham, in *Computer Applications in Applied Polymer Science,* 1982, No. 197, pp. 329–352.
33. J. B. Enns and J. K. Gillham, *Trends Polym. Sci.,* **2**(12), 406–418 (1994).
34. F. Parodi, C. Belgiovine, and C. Zannoni, U.S. Pat. 5,288,833 (Feb. 22, 1994) (to the EniChem SpA).
35. H. P. Mueller, J. Franke, and J. Sanders, *Adv. Urethane Sci. Technol.,* **12,** 166 (1993).